

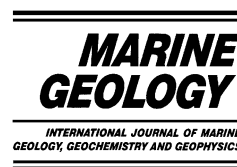


ELSEVIER

Available online at [www.sciencedirect.com](http://www.sciencedirect.com)

SCIENCE @ DIRECT®

Marine Geology 204 (2004) 251–272



[www.elsevier.com/locate/margeo](http://www.elsevier.com/locate/margeo)

# Shallow-marine phreatomagmatic eruptions through a semi-solidified carbonate platform (ODP Leg 144, Site 878, Early Cretaceous, MIT Guyot, West Pacific)

U. Martin<sup>a,\*</sup>, C. Breitkreuz<sup>a</sup>, S. Egenhoff<sup>a</sup>, Paul Enos<sup>b</sup>, L. Jansa<sup>c</sup>

<sup>a</sup> *TU Bergakademie Freiberg, Geology Department, Bernhardt von Cotta Str. 2, 09596 Freiberg, Germany*

<sup>b</sup> *Department of Geology, University of Kansas, 120 Lindley Hall, Lawrence, KS, USA*

<sup>c</sup> *Dartmouth, NS, Canada*

Received 25 June 2002; received in revised form 4 September 2003; accepted 21 November 2003

## Abstract

Leg 144 (1995) of the Ocean Drilling Program recovered basalts and volcanoclastic material from the volcanic basement of several guyots in the northwest Pacific, including MIT Guyot in site 878. Tectonic reconstruction suggests that this seamount originated as an intraplate volcano on the Pacific Superswell in the Early Cretaceous. Tephra emplaced by mass flow within the sedimentary cap is the subject of this study. The tephra unit consists of palagonitized, moderately to strongly vesicular basaltic clasts of apparent phreatomagmatic origin, carbonate mud- to grainstone clasts, and armoured lapilli. Armoured lapilli are inferred to have been formed during eruption within a steam envelope that developed above the vent due to magma–water interaction and high gas content of the magma. Another distinctive feature of the tephra unit are abundant truncation surfaces that cut the lithotypes due to subsidence, and are juxtaposed to the same lithotypes. These truncation surfaces are inferred to represent intra-eruption slip surfaces, which formed during eruption of the volcano that generated the tephra pile. The resulting slumps initiated grainflows and dilute turbidity currents, whose deposits are interspersed with those of high-concentration density currents. A subaqueous setting of deposition and eruption is indicated by the abundance of sideromelane glass shards, cauliflower-chilled clasts, the underlying marine carbonates, the lack of tachylite within the deposits, and sedimentary structures within the breccia.

© 2003 Elsevier B.V. All rights reserved.

*Keywords:* MIT Guyot; phreatomagmatism; armoured lapilli; atoll; Cretaceous

## 1. Introduction

Facies models for subaerial vs. subaqueous pyroclastic deposits have helped in interpretation of ancient deposits and their depositional and eruptive environments (e.g. Francis, 1982). Still, we often have difficulty in determining whether a particular ancient deposit formed subaerially or sub-

\* Corresponding author. Tel.: +49 (0)373-13811;

Fax: +49 (0)-373-13599.

*E-mail addresses:* [ulrike.martin@geo.tu-freiberg.de](mailto:ulrike.martin@geo.tu-freiberg.de) (U. Martin), [enos@ku.edu](mailto:enos@ku.edu) (P. Enos), [lubaj@cdut.edu.cn](mailto:lubaj@cdut.edu.cn) (L. Jansa).

aqueously. This study proposes a model for the formation of the pyroclastic material recovered from drilling the Cretaceous MIT Guyot, northwest Pacific, and a reconstruction of the volcanic event and its environmental setting. A high influx of pyroclastic material apparently occurred in a shallow marine setting. The paleoenvironmental reconstruction indicates the probability of entirely submarine eruption and deposition of the pyroclastic ejecta. The presence of abundant armoured lapilli within the tephra suggests development of

a sustained subaqueous eruption column and a water-exclusion zone (Kokelaar and Busby, 1992; White, 1996; Martin and White, 2000) in which vapor, juvenile material, carbonate clasts, and carbonate mud were transported upwards to form armoured lapilli.

Subaqueously formed successions have been studied (Gilbert, 1890; Cashman and Fiske, 1991; White, 1991; Fiske et al., 1998; Kano, 1998) but descriptions of shallow-marine eruptions through platform carbonates are lacking.

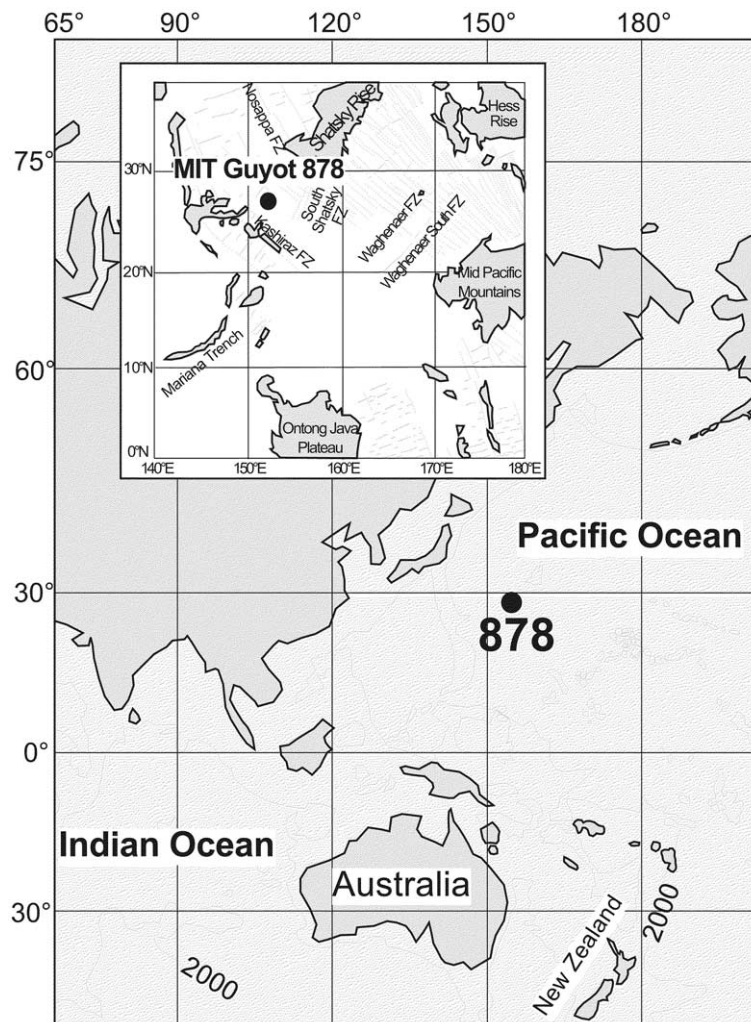


Fig. 1. Location of the study area in the northwest Pacific Cretaceous seamount province (modified after Shipboard Scientific Party, 1993).

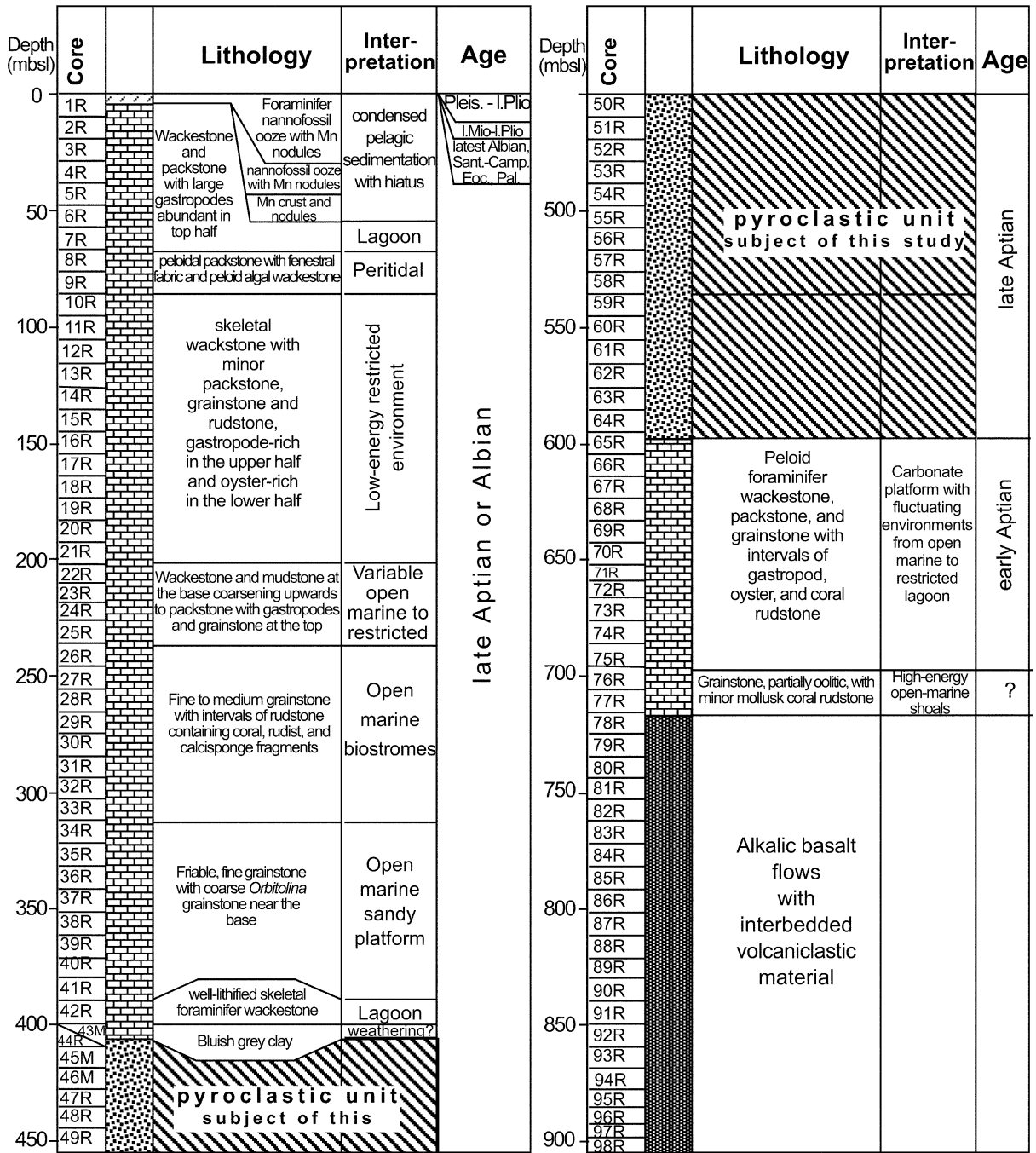


Fig. 2. Stratigraphic section of Site 878 (modified after Shipboard Scientific Party, 1993).

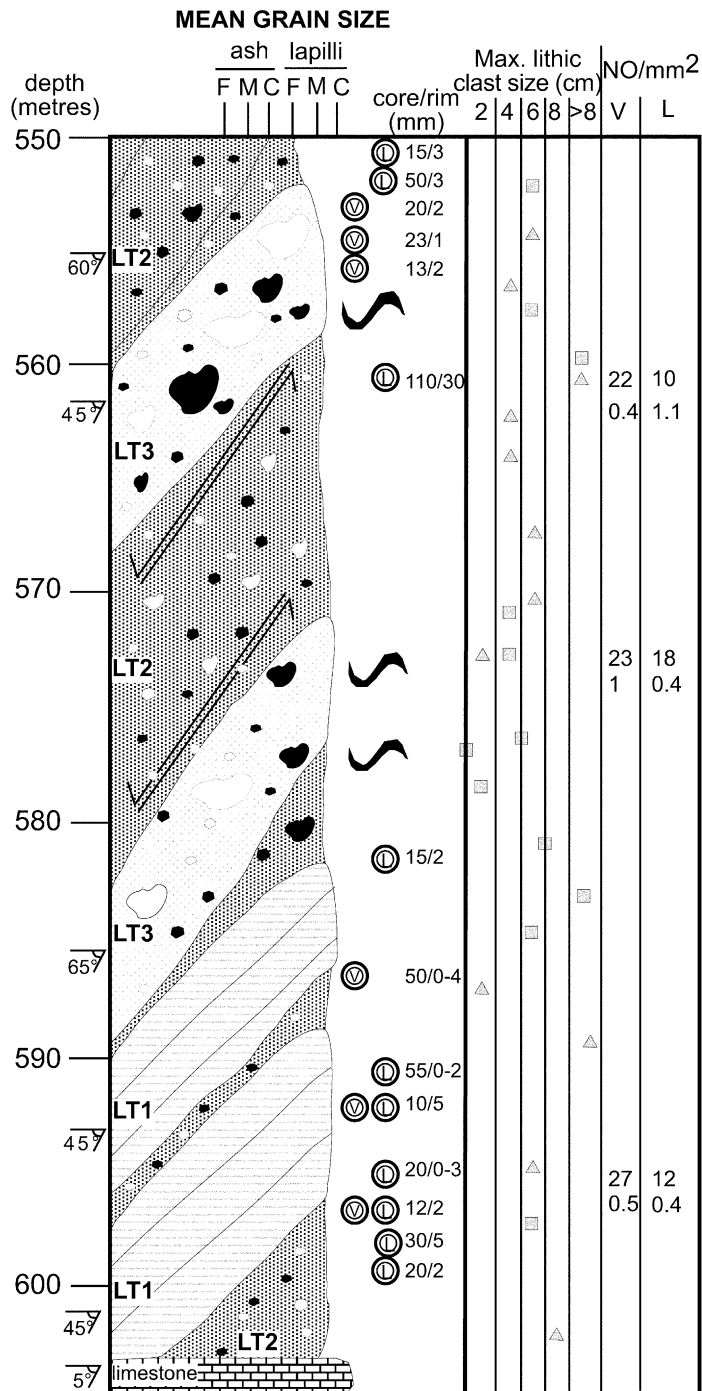


Fig. 3. Generalized lithologic log of the study interval. LT1 = Lithotype 1, LT2 = Lithotype 2, LT3 = Lithotype 3, LT4 = Lithotype 4. Lithotypes are explained in Table 1. Note: NO/mm<sup>2</sup> = number of clasts per mm<sup>2</sup>.

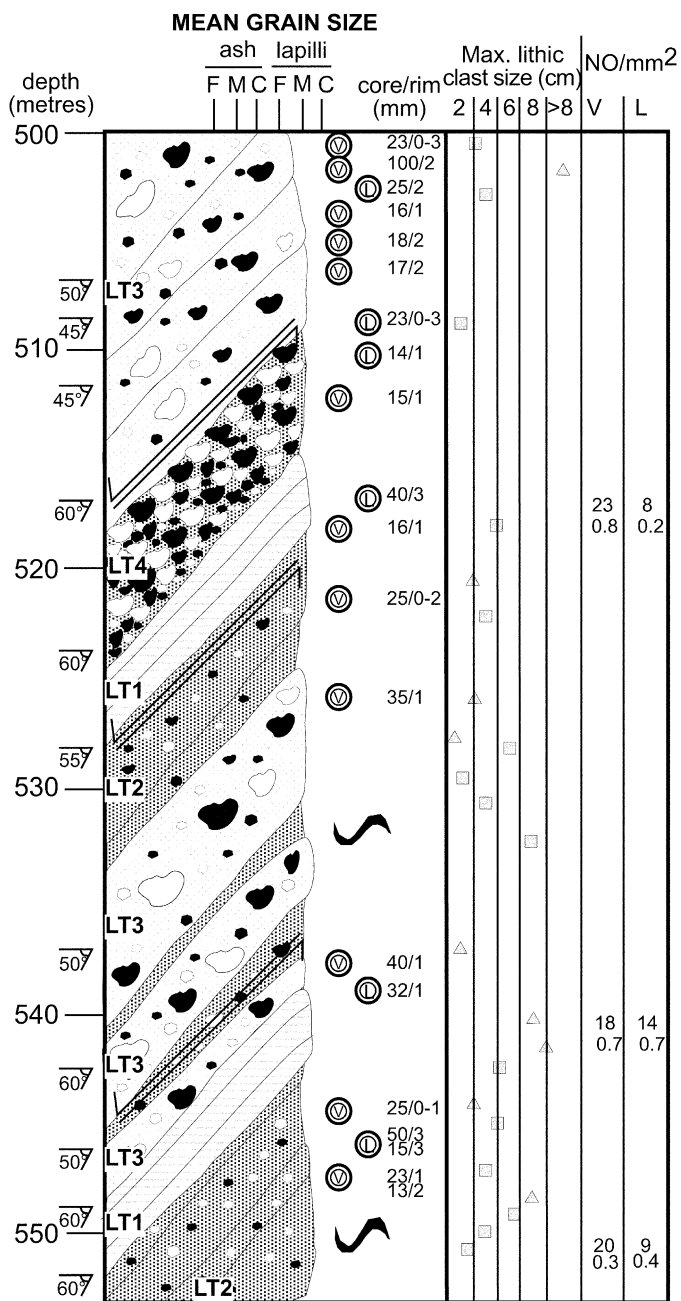


Fig. 3 (Continued).

In general, prior studies have concentrated on the morphology of seamounts, their ages, petrology, and total volume (cf. Winterer, 1976; Fornari et al., 1978; Batiza et al., 1984; Batiza, 1989;

Winterer et al., 1993; Rougerie and Fagerstrom, 1994; Bograd et al., 1997; Koppers et al., 1998; Caplan-Auerbach et al., 2000; Corcoran, 2000).

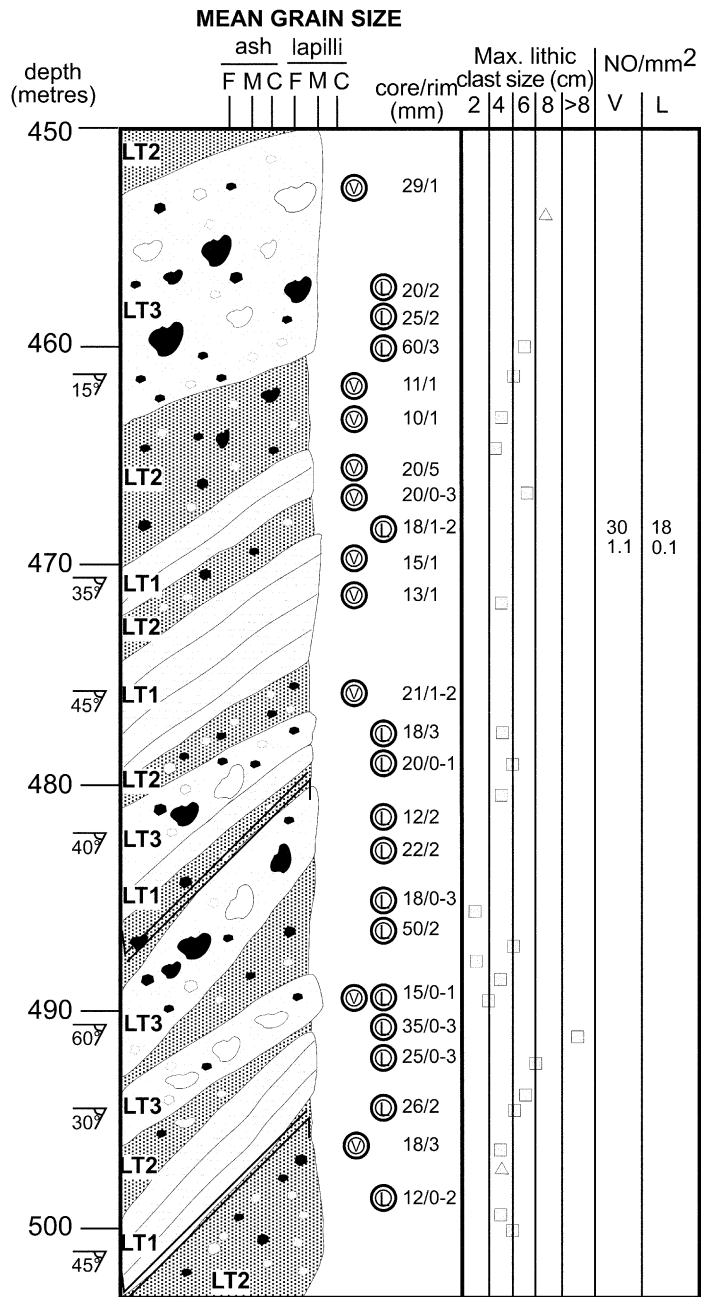


Fig. 3 (Continued).

**2. Geological evolution of the MIT Guyot**

Many of the submarine volcanoes of the north-west Pacific Cretaceous seamount province (Fig.

1) formed in a region of the South Pacific that is characterized today by the numerous island chains of French Polynesia and Samoa. It has been called the Pacific Superswell (McNutt and

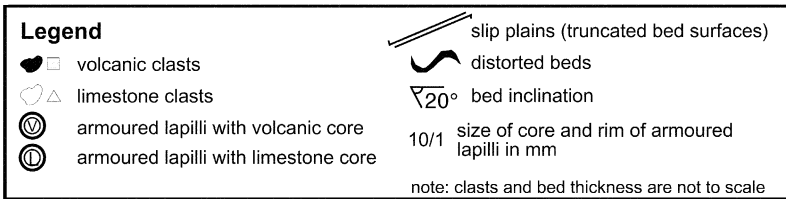
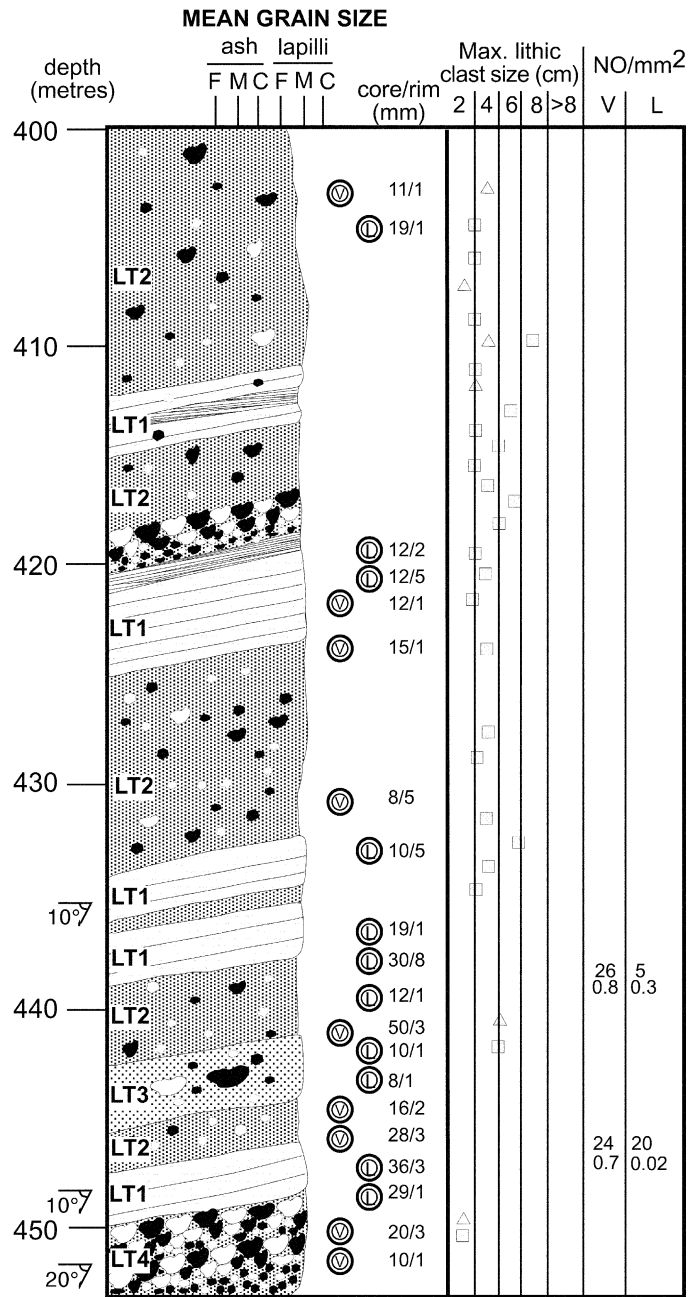


Fig. 3 (Continued).

Fischer, 1987; McNutt et al., 1990) or the South Pacific Isotopic and Thermal Anomaly (SOPITA; Smith et al., 1989; Staudigel et al., 1991).

A pre-site survey of the Massachusetts Institute of Technology (MIT) Guyot in the northwest Pacific led to the location of Site 878 at 27°19.143'N, 151°53.028'E in a water depth of 1323 m, on the northeastern part of MIT Guyot (Fig. 1). MIT Guyot is an isolated feature close to the Wake group in the 18–28°N guyot band (Shipboard Scientific Party, 1993). MIT Guyot was probably built over the Darwin Rise about 123 Ma, during the first of three constructional volcanic episodes (Winterer et al., 1993). Subsequent to the volcanic construction of the MIT edifice, a carbonate platform developed. The lower carbonate facies consists of pale brown foraminiferal and peloidal grainstone, packstone, and wackestone with minor rudstone rich in nerineid gastropods, oysters, and corals, indicating a restricted to open marine environment (Winterer et al., 1993; Shipboard Scientific Party, 1993; Jansa and Arnaud Vanneau, 1995; Ogg, 1995). However, only 6.5% of the lower platform material was recovered. Given this overall low recovery, precise relationships between different lithologies cannot be made.

In this paper we consider unit IV of Site 878 comprising polymictic breccia or lapilli tuff of late Aptian age (Jansa and Arnaud Vanneau, 1995) that contains both basalt and carbonate mud- to grainstone clasts from the underlying platform in a greenish-gray carbonate matrix (Fig. 2). Nearly 100% core recovery was attained through 204.6 m of the breccia that extends from 399.7 to 604.3 mbsf (Shipboard Scientific Party, 1993). The uppermost 12 m of the tephra are oxidized, formerly interpreted as the result of subaerial exposure before resumption of carbonate deposition (Ogg, 1995, p. 344). Two cm of dark greenish-gray, pyrite-rich clay recovered at the top of the breccia may represent a 7-m interval (Shipboard Scientific Party, 1993) or 70 cm (Ogg, 1995). It was variously interpreted as an altered volcanic layer (Shipboard Scientific Party, 1993) or as a restricted, marginal-marine, transgressive unit (Ogg, 1995). Two 10-cm intervals with very low resistivity within the top 4 m of the carbonate unit

that underlies the breccia are interpreted as volcanic ash layers that presaged the explosive eruption (Ogg, 1995, p. 343).

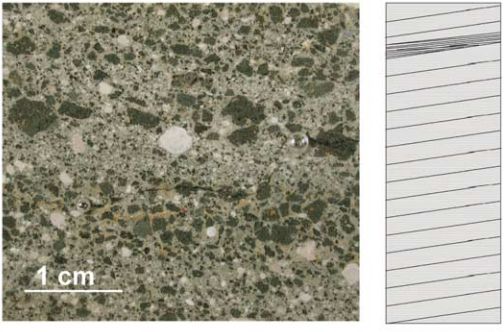
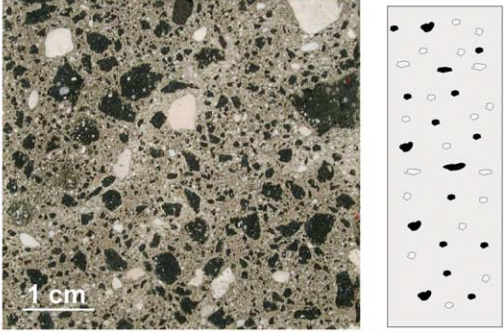
Previous descriptions of the breccias recognized two cycles of deposition (600–514 mbsf and 514–399 mbsf), based at least in part on color changes as reflecting the volcanic content (Shipboard Scientific Party, 1993; Ogg, 1995; Christie et al., 1995). Such a differentiation is not indicated by the core descriptions (Fig. 3) nor by the quantitative measurements (Fig. 5).

The recovered basement at MIT is 185 m of basalt formed by at least 24 lava flows consisting of three geochemically distinct groups separated by apparent weathering horizons (Christie et al., 1995; Holmes, 1995). The three groups are dated at 119.6±0.7; 121.7±1.6; and 122.8±0.2 Ma (Pringle and Duncan, 1995). The volcanics are extensively altered with both matrix and phenocrysts replaced by smectite and minor hydro-mica, chlorite, mixed layer smectite–chlorite (Kurnosov et al., 1995), kaolinite, goethite, and hematite (Holmes, 1995, p. 392), but the original structures are readily recognizable (Christie et al., 1995). The volcanic rocks were interpreted as subaerial lava flows based on well-defined vesicular and oxidized, brecciated flow tops that grade downwards into massive basalt (Christie et al., 1995; Holmes, 1995). Basalts are intercalated with volcanoclastic material, consisting of 3–4 breccias and 3 intervals of fine-grained, highly altered material with relicts of volcanic glass shards (Christie et al., 1995). Two of these units are interpreted as water-laid tuffs comprising poorly sorted, vesicular and non-vesicular volcanic clasts in a vitric matrix.

The volcanic breccia is overlain by 118 m of Aptian shallow-water platform carbonates (2.26% recovery), followed by the pyroclastic succession (204 m), which is subject of this study (Fig. 2). The pyroclastic sequence is succeeded by 396 m of late Aptian to late Albian shallow-water limestones and a miniscule pelagic cap with manganese nodules and mixed biota, about 3.2 m thick (Shipboard Scientific Party, 1993; Jansa and Arnaud Vanneau, 1995). Due to the low recovery of the platform carbonates the precise position of unit boundaries is not known.



Table 1  
Description and interpretation of the lithotypes

A	Litho type	Key to Fig. 3	Description	Inferred depositional process
	LT 1		<ul style="list-style-type: none"> <li>-normally, reverse, or symmetrically graded</li> <li>-undulating bedding contacts</li> <li>-bed thickness from 0.2 m to 1 m</li> <li>-alternation of matrix-rich and matrix-poor layers with differences in colors matrix-rich beds are darker than the matrix-poor</li> <li>-locally are well-developed low-angle cross bedding sets, thickness ranging from several cm to several tens of cm</li> <li>-matrix micritic with abundant, fine, dispersed, blocky sideromelane glass shards</li> </ul>	<p>Normally graded to ungraded, matrix-rich beds record traction deposition from dilute turbidity currents (Ta,c; Lowe, 1988).</p> <p>Matrix-poor, coarse-grained, inverse-graded beds suggest traction carpet sedimentation (S2; Lowe 1982).</p> <p>Graded and laminated thin divisions are interpreted as Ta-b turbidites (Lowe, 1988) They could have formed either as eruption-fed turbidity currents during the last stages of eruption or by later episodic remobilization.</p>
	LT 2		<ul style="list-style-type: none"> <li>-thick (dm scale), structureless, matrix-rich layers</li> <li>dark volcanic clasts and light coloured limestone clasts randomly dispersed</li> <li>-crudely developed beds locally defined by elongated sub-horizontal clasts (alignment bedding)</li> <li>-poorly sorted</li> <li>-matrix micritic with fine sideromelane glass shards</li> </ul>	<p>Rapid, high concentration suspension sedimentation (Chough &amp; Sohn 1990)</p>

### 3. Terminology and methods

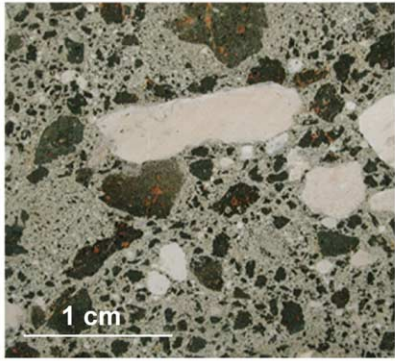
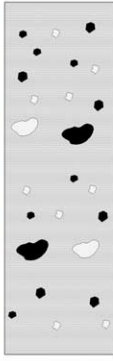
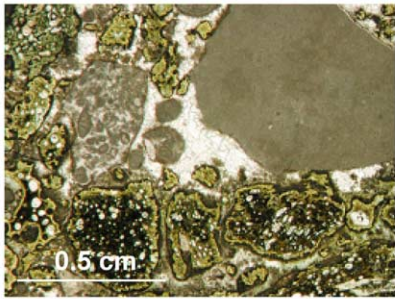
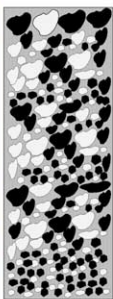
Units were distinguished in the core on the basis of sedimentary structures, volcanic textures, and the shape and size of pyroclasts. Terminology follows Fisher and Schmincke (1984), who defined pyroclastics as particles produced directly by volcanic processes without reference to the causes of eruption or the origin of particles. Volcaniclastic fragments include all clastic volcanic materials formed by any fragmentation process, dispersed by any transporting agent, deposited in any environment, or mixed in any significant proportion with non-volcanic fragments (Fisher, 1961; Fisher and Schmincke, 1984).

Semi-quantitative determination of size and abundance of clasts in 12 slabs is by image anal-

ysis using KS 300 Kontron Elektronik version 2.0. Particles ranging in size between 10 and 0.01 mm were measured and defined as clasts. The fraction (<0.01 mm) is defined as matrix and consists of carbonate mud (Elf-Aquitaine, 1975). We are aware that the 2-D cross sections do not really reflect the true size values, but the ratios bear only small mistakes by using 2-D instead of 3-D values. The volumetric proportion of clasts in a rock is equal to the area proportion of the clasts in any section (Delesse, 1847; Higgins, 2002).

All armoured lapilli have been quantitatively recorded by measuring diameters of cores and thickness of rims in core slabs. In most cases this was a 2-D observation. We assume that the shape of the armoured lapilli is rather regular so

Table 1 (Continued).

B	Litho type	Key to Fig. 3	Description	Inferred depositional process
LT 3			<ul style="list-style-type: none"> <li>-thick (dm scale), structureless beds with gradational contacts</li> <li>-clasts ranging from 2 mm to 2 cm</li> <li>-bedding apparent as changes in clast size</li> <li>-large limestone or volcanic clasts (&gt;3 cm) are concentrated in distinct layers, commonly near the center of the beds</li> <li>-micritic matrix (20 - 30 vol%)</li> <li>-poorly sorted</li> </ul>	<p>High-concentration density current in which the large volumes of sediment, ejected from the vent, suppressed turbulence (Fisher et al., 1987; Valentine, 1987; Schumacher and Schmincke, 1991). Large floating lapilli suggest that the inertial layer was in a quasi-static framework and was able to transport the lapilli along the top or within it (Postma et al. 1988).</p>
LT 4			<ul style="list-style-type: none"> <li>-clast-supported</li> <li>-reverse graded</li> <li>-space between clasts generally cemented by calcite sparite</li> <li>-thickness ranges in cm-scale</li> <li>-contacts to overlying and underlying beds are gradual</li> <li>-maximum grain size is about 2 cm</li> <li>-moderate sorting</li> </ul>	<p>Deposition from grain flows, which may have originated from instantaneous remobilization of fallen pyroclasts (Cough &amp; Sohn 1990). Inverse grading resulted most likely from dispersive pressure within a shearing, high-concentration suspension or a traction carpet driven by a turbulent and dilute overriding surge (Cough &amp; Sohn 1990)</p>

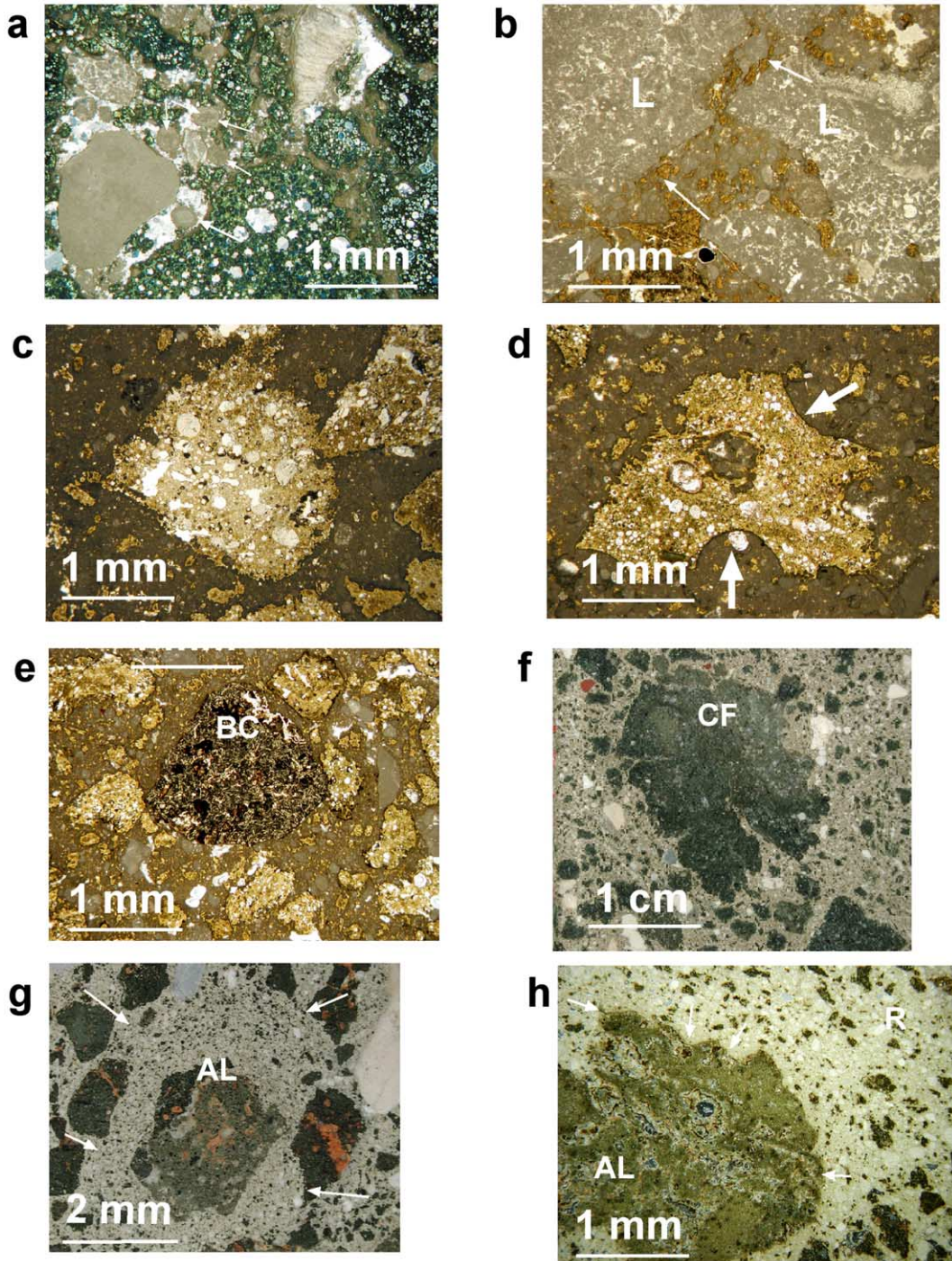
that the error is minimal. Bedding dips were measured directly from the core during qualitative core description at the ODP core repository.

#### 4. Lithotypes

Four depositional lithotypes, LT1 through LT4,

are recognized in the core (Table 1, lithotype summary and interpretation; Fig. 3, core log). Lithotype 2, thick, structureless layers with randomly dispersed dark volcanic clasts and light carbonate mud- to grainstone clasts, is the most common and conspicuous facies; it occurs in all levels in the core. In contrast, lithotype 3, similar in appearance with larger clasts, is more common

Fig. 4. (a) Light-gray carbonate clast in micritic matrix. Note the abundant ooids around the carbonate clast (arrows); photomicrograph, plane-polarized light. (b) Semi-lithified lime packstone clasts (L). Note the irregular margins of the clasts (arrows), which suggest eruption through a semi-lithified carbonate platform rather than due to reworking in the vent; photomicrograph, plane light. (c) Highly vesicular sideromelane clasts. Note the large, round and irregular vesicles; photomicrograph, plane light. (d) Sideromelane glass shard with well-developed bubble-wall structure (arrows) and abundant vesicles; photomicrograph, plane light. (e) Microcrystalline basalt clasts (BC), interpreted to be derived from underlying basalt lava flows; photomicrograph, plane light. (f) Cauliflower-textured (CF) sideromelane clasts with chilled, cracked, and irregular margins surrounding a more highly vesicular interior; polished slab. (g) Well-developed armoured lapillus (AL). Note that the particles in the rim are concentrically arranged around the core (arrows), polished slab. (h) Segment of an armoured lapillus (AL). Note the core is formed by a cauliflower-textured sideromelane clast (arrows). Rim (R) is formed by ash-sized sideromelane and carbonate clasts; photomicrograph, plane light.



lower in the core, between 550 and 590 mbsf, but occurs locally also at higher levels. Lithotype 1, thinner, normal- or reverse-graded beds, alternating between matrix-rich and matrix-poor, is predominant between 590 and 600 mbsf, but also alternates with all the other lithotypes at various levels. Lithotype 4, thinner, but coarser grained, clast-supported, reverse-graded beds, is least common; it occurs at 420, 450, and 520 mbsf (Fig. 3).

The matrix of the breccia is carbonate-rich throughout, with varying admixtures of altered glass shards. Lime mud is the dominant component, but peloids, pisoids (2–5 mm in diameter), ooids, foraminifera, bivalve fragments, and other biota occur in most samples (Fig. 4a,b) (Shipboard Scientific Party, 1993, p. 1031; Jansa and Arnaud Vanneau, 1995, table 1). Peloids comprise up to 45% of some samples, and ooids are locally 30% of the volume.

Bent and truncated bed contacts are common

in the breccia. Distorted beds occur in many levels of the succession, suggesting post-depositional deformation from loading or from steam and water escape. Many small-scale faults observed in the core are attributed to syn-eruptive slip failure. Similar breaks are reported as characteristic in the evolution of Surtseyan volcanoes (Kokelaar and Durant, 1983; Lorenz, 1974; see below). The dip angles of the various types of surface generally increase with depth in the core, from 10° near the top to as much as 60° at the base (Fig. 3).

### 5. Clast types

Three types of clasts predominate in the breccia: (1) carbonate mud- to grainstone clasts; (2) volcanic clasts, and (3) armoured lapilli. In the lower part of the core (540 to 600 mbsf) the pro-

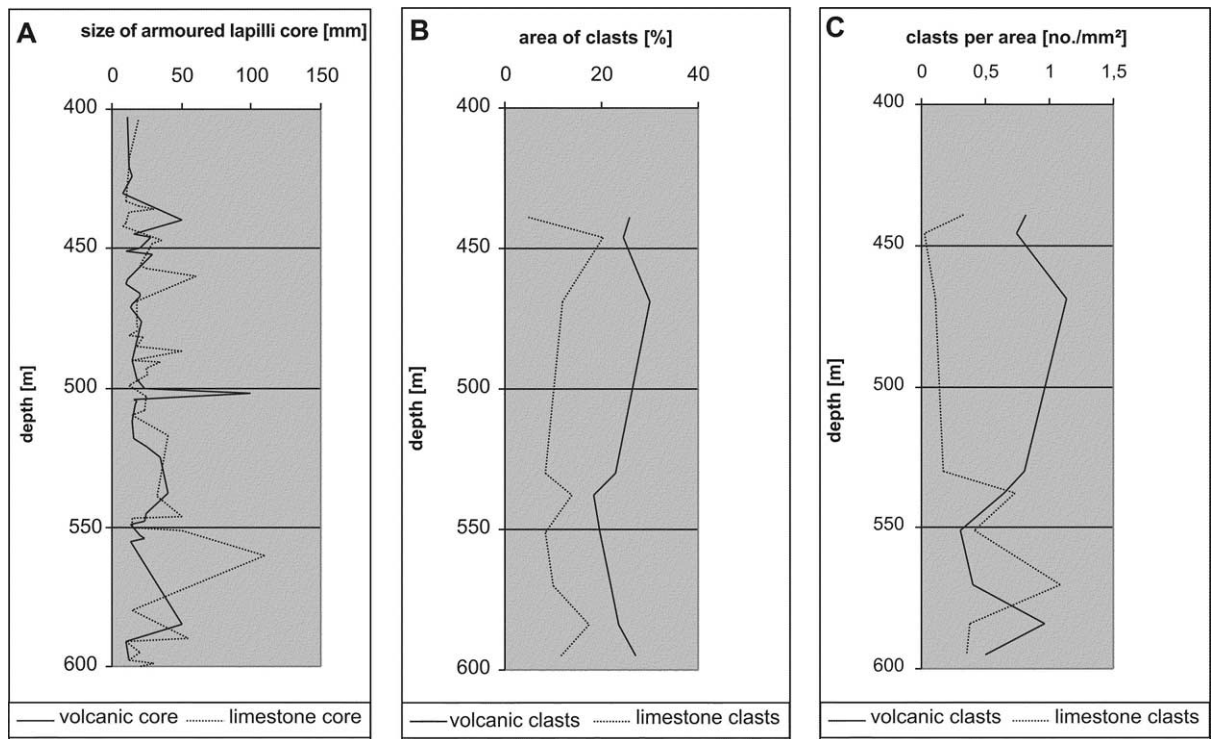


Fig. 5. Clast size. (A) Core size (volcanic or carbonate) of armoured lapilli plotted against depth in core. (B) Percentage of core area occupied by volcanic and carbonate clasts. (C) Abundance of clasts per unit area of core. Quantitative determinations in (B) and (C) are by image analysis using KS 300 Kontron Elektronik version 2.0.

portion of small limestone clasts is relatively high in comparison to the rest of the core, whereas the proportion of volcanic clasts increases toward the top of the core (Fig. 5B). This is consistent with the abundance of limestone-cored armoured lapilli in the lower part of the core (Fig. 5A). The largest carbonate clasts are at about 450 mbsf (Fig. 5C).

### 5.1. Carbonate mud- to grainstone clasts

These clasts are easy to identify due to their whitish color (Fig. 4a). Dominant limestone lithologies are mudstone, wackestone, and peloid or ooid pack- to grainstones. Locally small benthic foraminifera, bivalve fragments, or vuggy porosity is present. The carbonate clasts are generally rounded to subangular or have irregular, broken and fluidal margins (Fig. 4a,b).

#### 5.1.1. Interpretation

The abundance of carbonate mud- to grainstone clasts and the calcareous matrix, as well as the juxtaposition of the breccia on platform carbonates, clearly demonstrates renewed eruption of the volcanic pedestal through its carbonate cap, following perhaps 4 m.y. of dormancy (dates from Pringle and Duncan, 1995).

Carbonate mud- to grainstone clasts with irregular and broken margins, especially in grain-supported textures that lack intergranular cohesion (Fig. 4b), indicate partial consolidation of the platform carbonates before the first eruption. Reworking in the vent may have produced the rounded clasts. The prevalence of lime mud and isolated carbonate particles in the matrix suggests penecontemporaneous volcanism and sedimentation.

### 5.2. Volcanic clasts

The volcanic clasts can be subdivided petrographically on the basis of vesicle abundance and composition. The subtypes are: (1) microcrystalline basalt clasts (Fig. 4e), which are very rare (less than 1% total volume); (2) low-vesicular sideromelane clasts; and (3) highly vesicular volcanic clasts (Fig. 4c) formed by sideromelane,

which are commonly angular to sub-rounded. Vesicle diameters show a wide range; some vesicles are stretched into tubes; coalescence of vesicles is common. Locally zeolites fill vesicles. No tachylite (opaque glass) was observed in the core.

Both types of sideromelane glass shards locally contain microliths. Sideromelane grades from almost fresh glass, through particles with palagonite rims, to fully palagonitized tephra in which a pervasive pseudomatrix of zeolites and clays has completely filled the vesicles or even replaced entire beds. Sideromelane glass shards locally show bubble-wall structures (Fig. 4d). Clast size varies from a few mm to several cm. Almost all volcanic clasts are angular to sub-angular; a few are sub-rounded. Typically lapilli-sized clasts are angular, whereas larger ones are sub-angular to sub-rounded. Larger clasts lie sub-horizontally without any impact sags. Some larger fragments show chilled, cracked, and irregular margins surrounding a more highly vesicular interior (Fig. 4f); such fragments have been called ‘cauliflower bombs’ (Lorenz, 1973).

Quantitative analysis of the clasts shows that the volume of volcanic clasts was rather constant during eruption (Fig. 5B), but that the size of clasts increased upward from 600 to 550 mbsf and then decreased toward the top (Fig. 5C).

#### 5.2.1. Interpretation

Sideromelane clasts in the samples are interpreted as juvenile, the result of phreatomagmatic interaction of basalt and water. Microporphyrific basalt clasts are interpreted as accidental clasts derived from underlying lava pile (cf. Christie et al., 1995). Coalescing vesicles in the sideromelane clasts generally suggest significant bubble nucleation prior to eruption. The abundance of spherical vesicles is consistent with vesiculation at shallow depths near the vent (Heiken and Wohletz, 1991). Different vesicle shapes commonly imply variable lava viscosity and internal shear. The wide variation in abundance of vesicles found in the clasts probably reflects complex variation in the relative timing of vesicle formation and water-induced fragmentation. Magma–water interaction at an early stage greatly reduces the vesicularity

index and broadens the size range. Late-stage interaction, in contrast, has only minimal effect on the index and broadens the size range to only a limited extent (Houghton and Wilson, 1989).

Shards formed by cracking due to thermal shock are typically glassy and lack vesicles. However, many tuffs associated with maar and tuff-ring deposits include shards that range from vitric to slightly to highly vesicular (White, 1991, 1996). Such variety apparently results from a combination of vesiculating magma and quenching by water or steam. Deposits of such shards, which may show all transitions from blocky through slightly vesicular with scalloped edges to highly vesicular, are characteristic of shallow-water eruptions (Fisher and Schmincke, 1984). They are reportedly the most common type of ash produced underwater and typically occur in seamounts and in the transition from seamount to oceanic island (Fisher and Schmincke, 1984).

The presence of cauliflower bombs indicates contact with water during fragmentation (Lorenz, 1973). The larger chilled cauliflower-margins are inferred to have chilled abruptly upon leaving the gas-thrust column, initially at the column margin and later, for some of the larger clasts, during aqueous transport.

Elongated vesicles in the sideromelane clasts formed in response to shear of vesiculating magma against the walls of the vent (Fisher and Schmincke, 1984; McPhie et al., 1993). The roundness of the larger clasts is probably not a result of abrasion, but results instead from shaping of molten clasts by surface tension. The paucity of reworked and abraded clasts suggests ongoing deposition directly from an eruption column.

Abundant sideromelane is thus a criterion for recognizing basaltic magma quenched by external water. The mixture of well-preserved, clear sideromelane pyroclasts with palagonitized ones, in contrast, suggests recycling of pyroclasts within the vent (White, 1991).

The increase in size of volcanic (and carbonate) clasts from 600 to 550 m-bsf in the MIT succession (Fig. 5C) is interpreted to reflect declining fragmentation efficiency after the initial contact of water and magma. Fragmentation efficiency

rose again at a later stage when the vent was cleared of carbonate mud (Fig. 5).

### 5.3. Armoured lapilli

Armoured lapilli with carbonate cores dominate some segments within the breccia, whereas others are dominated by volcanic rock cores (Figs. 3 and 5A). Most of the lapilli are well rounded; many are spherical; others are slightly oval or elliptical. The armoured lapilli have cores of lapilli-sized and block-sized rock fragments (2–64 mm; Fisher, 1961) concentrically coated by carbonate mud mixed with ash-sized sideromelane glass shards (Fig. 4g,h). Cores are formed either by carbonate clasts (commonly mudstones) or by vesicular sideromelane glass shards, exceptionally with cauliflower-texture (Fig. 4h). Variation is great in the size of cores (10–110 mm) as well as thickness of rims (1–30 mm). The core size and rim thickness of all armoured lapilli were measured (Fig. 2). Diameter of volcanic and carbonate cores is plotted as a function of depth in Fig. 5A.

#### 5.3.1. Interpretation

Armoured lapilli are a type of accretionary lapilli composed of a crystal, pumice, or lithic fragment core which is surrounded by a rim of fine to coarse ash (McPhie et al., 1993). They are common in the geological record, particularly in facies of phreatomagmatic eruptions that generated abundant fines (Fisher and Schmincke, 1984). However, armoured lapilli within MIT deposits are unusual because cores are coated mainly by carbonate mud and minor coarse ash particles. This is facilitated by the high incorporation of carbonate mud into the eruption cloud. Armoured lapilli are generally considered to be restricted to the proximal facies (Schumacher and Schmincke, 1991). Although armoured lapilli commonly have been used to identify subaerially erupted tephra, recent studies (e.g. White and Houghton, 2000) show that their formation is also possible in subaqueous settings within the steam envelope of the eruption column. Condensation of steam during outflow of pyroclastic mass flows and wet carbonate clasts promote

early, thick coatings of ash on the coarser clasts. The presence of armoured lapilli throughout the MIT breccia indicates continued incorporation of unconsolidated lime mud into the erupting vent (cf. White, 1991).

## 6. Submarine vs. subaerial eruptive and depositional environment

Although most of the described features may also form in a subaerial setting due to magma–water interaction, we suggest a submarine setting for the following reasons. (1) Most of the beds are massive and do not resemble typical base surge deposits but rather subaqueous mass flow deposits. Fisher (1977) for example reported from deposits of Koko Head (Hawaii) that they are well bedded, dune- and cross-bedded, all features which are missing at MIT deposits. In contrast, transitional, subaqueous deposits of Tok Island (Korea) have been described as thick-bedded, massive or inversely graded beds (Sohn, 1995). At Koko Crater (Hawaii), where slumping of oversteepened slopes played a major role during formation, clear evidence of magma–water interaction is lacking as a result of isolation of the active vent from sea water (Knight et al., 1987). (2) The whole sequence shows a more or less similar composition without any changes in the appearance of volcanic glass (sideromelane vs tachylite). Tachylite is basaltic glass that is highly charged with Fe and Ti-oxides, and therefore nearly opaque, whereas sideromelane is commonly transparent. The formation of volcanic glass is mainly dependent on the cooling rate of the melt and the viscosity of a stable silicate liquid (Fisher and Schmincke, 1984). When a silicate melt is cooled rapidly below its crystallization temperature, it first forms a supercooled liquid and then a solid amorphous substance, volcanic glass (Carmichael, 1979). The composition of volcanic glass, therefore, represents the initial composition of the melt. The cooling rate determines which variety of glass, tachylite or sideromelane, is formed. Slow cooling allows Fe and Ti oxide crystallites to form, thus favoring tachylite. Therefore, it is commonly more abundant in the emer-

gent part of Surtsean volcanoes. Lack of tachylite together with the high vesicularity of the glass shards indicates shallow subaqueous eruption (Staudigel and Schmincke, 1984). Water has a much higher heat capacity and conductivity than air (Carslaw and Jaeger, 1947) and thus absorbs large quantities of vaporization heat. As a result, cooling rates at magma/water contacts are much higher than where lava erupts in air. The volcanic breccia is overlain by waterlain tuff (today altered to mud).

Deposition of the MIT sequence, therefore, either took place completely subaerially where somehow cooling rate of the melt was exceptionally high and/or subaerial part has been destroyed by erosion, or completely subaqueously. We favor the latter possibility, because in all known subaqueous to emergent volcanoes there is a significant change in the sequence from subaqueous to emergent generated deposits (e.g. Sohn and Chough, 1992; Sohn, 1995; Belousov and Belousova, 2001). Underlying carbonate platform sediments suggest fluctuating environments from open marine to restricted lagoon, therefore it is likely that eruption took place during marine high-stand after subsidence of the carbonate platform.

## 7. Carbonate sedimentology – defining the palaeodepth of the lagoon

The contact of the early Aptian carbonate unit with the overlying volcanic breccia is formed by mud-free grainstones. If it is assumed that these sediments really represent the surface deposits at the time of the volcanic event, palaeowater depth would have been in the range of only a few meters. It is therefore unlikely that the water column covering the lagoon during the explosion was sufficiently thick to produce an entirely submarine eruption. However, several lines of evidence support a water–magma interaction within the sedimentary column.

The uppermost layers preserved in the core below the breccia are composed mainly of carbonate sands. The bulk of carbonate incorporated in the breccia, in contrast, consists of lime mud. The breccia is about 200 m thick covering the entire

buildup. Even if a part of the inner lagoon during the explosion was filled with lime mud, its volume was surely not enough to explain the amount of fine-grained carbonate incorporated in the breccia.

Besides the mud, also angular clasts of well lithified parts of the succession occur in great abundance within the volcanic breccia. This argues for the incorporation of a significant amount of buried Aptian rocks during the explosion. Large amounts of still unlithified carbonate mud intercalated with lithified beds form the inner part of the lagoonal succession (Ogg, 1995). It is likely that these pore spaces were filled with marine water during the Aptian explosion. This is also indicated by rims of equally grown early calcite cements around sand-sized grains throughout the cored interval. For a maximum of 120 m overburden between 40 and 50% of pore space is envisaged for carbonate muds (see compilation of several sources in Goldhammer, 1997). The pore volume in carbonate sands at a depth of 120 m is about the same (40–60%). However, only the basal layers of the studied locality should have had these porosities, most of the succession would show a higher water content due to less pronounced compaction. With an average of 50% of water-filled pores and a depth of no more than 120 m below sea level, it is most likely that the explosion occurred within the only partly lithified succession. In case of a strong reworking of parts of the succession during the volcanic event, however, the original early Aptian sedimentary column could have been significantly thicker. With an overburden of some 300 m more as will be discussed later in this study, the porosity values decrease, but according to Goldhammer (1997) for both carbonate sands and muds a primary porosity of around 40% is still present.

The recovered rock samples show only a minor content of reworked reef-derived algal facies and coral debris. Therefore, the drilling must have perforated lagoonal facies situated in some distance from the back-reef sand shoals of the early Aptian carbonate platform. It is, however, unclear if the palaeobathymetric position of the drilling is comparable to the part of the lagoon where the explosion took place. Whether a 4-m-thick grain-

stone package that formed the uppermost Aptian carbonate layers preceding the volcanic event was present in the locality where the eruption took place is speculative. The high mud content in the breccia and the comparatively small number of carbonate grain clasts rather supports eruption within more mud-dominated lagoonal sediments.

Furthermore, a single well may not fully reflect the evolution and geometry of this buildup. It remains unclear how much unconsolidated sediment on the platform top has been removed and incorporated in the breccia. In contrast to the model proposed by Ogg (1995), it is possible that the explosion affected the platform during a relative sea-level highstand with widespread mud-dominated facies. In this case, the explosion could have led to the removal of the uppermost carbonate layers. The preserved contact between the carbonates and the breccia would then represent a surface within the sedimentary column that does not at all reflect the sedimentary conditions at the time of the volcanic event. As large parts of the early Aptian sediments, especially the mud-dominated facies, show little cementation even today (Ogg, 1995), the explosion might have removed preferentially the mud and left behind more cemented grainstones that form the contact today.

Ogg (1995) suggests that the uppermost grainstone beds preceding the eruption reflect a relative sea-level lowstand. However, as discussed above, the eruption might have occurred during a sea-level highstand, and indeed the great amount of carbonate mud incorporated in the volcanic breccia rather supports this hypothesis. A correlation of the sea-level changes observed within the MIT Guyot with the Haq et al.-curve (1987) is not envisaged. Biostratigraphic resolution is poor, and the recovery rate so low that the sea-level interpretations by Ogg (1995) are largely speculative. It has to be stressed, however, that the restricted data base does not allow for better reconstructions. It should further be kept in mind that for the Cretaceous, correlation of individual sequences is problematic even with better time control (Miall, 1992), especially when the study area is situated on a still active magma chamber that might control subsidence or uplift.



## 8. Discussion

Each of the four lithotypes recognized at MIT Guyot is attributed to deposition from density currents (Table 1). The emplacement of high- and low-concentration pyroclastic density currents in subaqueous settings has been documented widely (Fiske and Matsuda, 1964; Cashman and Fiske, 1991; Nishimura et al., 1992; Kokelaar and Busby, 1992; White, 1996; Kano, 1996; Smellie and Hole, 1997; Fiske et al., 1998) but reports on eruption within an atoll appear limited to the MIT Guyot (Shipboard Scientific Party, 1993; Christie et al., 1995; Ogg, 1995). Abundant carbonate mud- to grainstone clasts and calcareous matrix in the breccia demonstrate that eruption occurred through the underlying platform

carbonates. Carbonate clasts with irregular and broken margins indicate that at least portions of the carbonates semi-lithified prior to eruption. Fragmentation of lithified carbonates and rounding by reworking in the vent or during transport appears less likely.

The distribution of the clasts within the succession is interpreted to reflect differences in eruption style or differences in eruption locus. The large number of small carbonate clasts in the lower part of the core suggests initial phreatomagmatic interaction of magma with water-saturated, semi-solidified carbonate. In the process of eruption, the vent area was cleared and magma–water interaction gradually led to the formation of more juvenile clasts, as shown by an increase of volcanic clasts toward the top of the breccia (Fig. 5C).

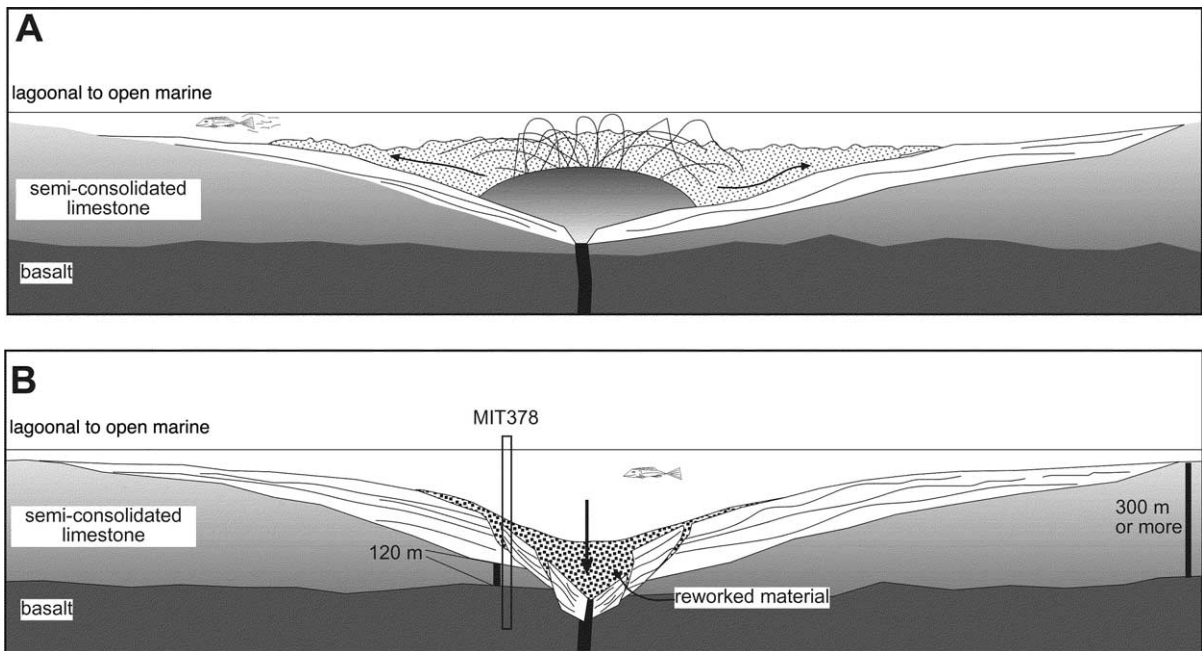


Fig. 6. Schematic illustration of inferred processes of eruption on MIT Guyot (modified after White and Houghton, 2000). (A) Early subaqueous jetting due to interaction of magma and wet sediment. Explosions and collapsing jets produced dilute, turbulent, gravity flows containing mainly juvenile material. Deposition took place mainly from traction (LT 1), but occasional ejection of the vent slurry or collapse of unusually concentrated tephra jets formed a highly concentrated dispersion that deposited LT 2. Vigorous, more sustained volcanic activity formed a steam envelope in which clasts were transported partly by steam expansion, resulting in deposition of massive beds (LT2 and LT3) and armoured lapilli. Fragments of consolidated marine carbonate and abundant carbonate mud resulted from quarrying into the seafloor during this activity. (B) Subsequent and post-depositional subsidence triggered failure of the vent wall producing slumping and remobilization of tephra into the vent, which resulted in deposition of LT 1 and LT 4.

Renewed eruption on MIT Guyot began in a very shallow marine setting as indicated by a general shoaling upward trend in the underlying carbonates, capped by oolitic grainstone just beneath the breccia (Shipboard Scientific Party, 1993; Jansa and Arnaud Vanneau, 1995). However, the present platform surface most likely was not the original surface during eruption (Fig. 6). Eruption gradually built a submarine edifice towards sea surface (Fig. 6). Immediately adjacent to the vent site, lithotypes 2 and 3 accumulated during ‘continuous uprush’ eruptive phases (termed continuous uprush by Thorarinsson et al., 1964; Thorarinsson, 1967; Kokelaar, 1986; Kokelaar and Durant, 1983; White, 1996). However, the development of a high eruption column most likely was suppressed by the lithostatic pressure of the platform carbonates (Fig. 6). It is inferred that eruption excavated a broad bowl-shaped depression in which eruption-fed currents moved laterally and deposited inside this depression, as reported by Belousov and Belousova (2001) during a phreatomagmatic eruption in Karymskoye Lake (Kamchatka, Russia).

Lithotypes 2 and 3 grade upward into relatively steeply dipping beds of a submarine crater (Fig. 6). The unusual matrix of carbonate-mud and the abundance of sideromelane glass shards suggest initial eruption within a semi-solidified carbonate platform that supplied the developing submarine eruption column with abundant carbonate mud and clasts and led to the formation of armoured lapilli in a submarine setting.

The apparently high gas content of the erupting magma, indicated by the abundant vesicles, promoted the formation of a subaqueous eruption column through explosive interaction of steam driven by highly energetic magmatic injections. This process is further indicated by the presence of armoured lapilli throughout the breccia, signaling continued incorporation of fluid carbonate mud into the erupting vent and development of a sustained subaqueous steam envelope. The steam condensed during outflow, promoted the early deposition of ash, and resulted in the coarser pyroclasts and lithoclasts being thickly coated with ash and mud.

Several lines of evidence, taken together with

the sedimentary structures of the deposits, strongly indicate subaqueous eruption and deposition: (1) the great abundance of sideromelane glass shards and carbonate clasts with the virtual exclusion of other clast types; (2) the lack of tachylite; (3) the cauliflower-chilled clasts as cores of the armoured lapilli; (4) the overlying waterlain tuff; (5) subsequent marine-carbonate deposition, beginning with a possible deeper water facies (Jansa and Arnaud Vanneau, 1995, p. 322); and (6) ‘accidental’ volcanic fragments are very rare in the breccia in comparison to the carbonate clasts. This indicates less vigorous fragmentation of the basalts beneath a few hundred meters of carbonate, thus a shallow fragmentation locus compared to typical subaerially formed successions.

Signs of significant pauses in sedimentation, wave-generated structures, or weathering episodes within the breccia are lacking. The red-stained interval in the top 12 m of the breccia is here interpreted as low-temperature hydrothermal alteration due to cooling of the erupted products or hydrothermal venting. Red-brown coloration has also been reported from oxidation of volcanics in shallow water (Staudigel and Schmincke, 1984). Volcanic glass is particularly susceptible to alteration because it is thermodynamically unstable and decomposes more readily than associated mineral phases (Fisher and Schmincke, 1984). Conversion of sideromelane to palagonite involves the addition of 18–30 wt% water, oxidation of iron, and loss of calcium and sodium (Peacock, 1926). All of these changes, except perhaps the loss of sodium, could occur readily in sea water. In contrast, Ogg (1995, p. 344) interpreted the oxidized interval to indicate that vertical accretion of tephra had formed a large island. Vertical accretion of tephra to form a positive volcanic form is unlikely, because subaqueous eruption within a soft-sediment environment is more likely to produce a ‘negative’ form (i.e. a crater) rather than a constructive volcanic form (Fig. 6; Belousov and Belousova, 2001).

As eruption continued, the steeply dipping sides of the crater produced high-concentration density flows that deposited lithotypes 2 and 3. Slumps from the accreting edifice initiated grain-

flows (lithotype 4) and dilute turbidity currents. Tephra was partly recycled by subsequent eruptive bursts, to mix highly palagonitized sideromelane glass shards with fresh ones (cf. Kokelaar and Durant, 1983). Abrupt changes in dip inclination within the breccia reflect failure and slumping due to subsidence, as does the presence of curved contacts and truncated beds (Figs. 3 and 6).

The location of the drill site within the vent, as opposed to a position on the flank of the volcano, is supported by the presence of the slip surfaces (Figs. 3 and 6), steeply dipping beds (Fig. 3), and the overall sedimentological aspects (Table 1). A steep paleo-surface on the outer edge of the carbonate platform where the erupted tephra could have accumulated, as suggested by Christie et al. (1995), appears excluded by the sub-horizontal attitude of the underlying platform carbonates, indicating a subhorizontal paleo-surface, as shown by the site seismic profiles (Fig. 3; Shipboard Scientific Party, 1993, pp. 343–4; note that the drill hole may have deviated about 5° from vertical), as well as the location of the site 1.3 km from the present slope break. The slope angles of MIT Guyot are typical of seamounts, 15–30° (Battiza et al., 1984), probably too steep to allow deposition of clastic materials. Most debris would have traveled to greater depths to build clastic aprons around the seamount. Thus, only the summit region, where slopes were far below the natural angle of repose, would be mantled by pyroclastic material. The steeply dipping beds, up to 60°, in the cores cannot be explained by depositional processes alone. Fault surfaces indicate failure; they are here interpreted as intra-eruption slip surfaces within the main vent or within a satellite vent, which are common in the summit region of a seamount (Staudigel and Schmincke, 1984). The generation of fault surfaces by uplift through pre-eruption bulging appears excluded. Such uplift would also affect the underlying sediments, which presently dip less than 5° (such apparent dips probably reflect hole deviation; cf. Shipboard Scientific Party, 1993). Dips decrease dramatically in the upper 50 m of the breccia (Fig. 3) and the overlying platform carbonates are horizontal.

## 9. Conclusions

Examination of the drill core and data from MIT Guyot (Fig. 3; Table 1) allow the reconstruction of a unique submarine eruption through a semi-solidified carbonate platform. It records a sequence of eruptive and sedimentary events otherwise typical of those which shape marine volcanoes of island arcs (Hoffmeister et al., 1929), shallow spreading ridges (cf. Richards, 1959), and coastal intra-plate settings (cf. Martin and White, 2000).

Inferred processes recorded in the MIT core were triggered by eruption that produced early subaqueous jetting due to interaction of magma with water-saturated sediment (Fig. 6A). Subsequent explosions and collapsing jets produced dilute, turbulent gravity flows containing juvenile material. Deposition took place mainly from traction (LT 1), but occasional ejection of the vent slurry or collapse of unusually concentrated tephra jets formed highly concentrated dispersions that deposited LT 2. More sustained, vigorous volcanic activity formed a steam envelope in which clasts were transported partly by steam expansion, resulting in deposition of massive breccia beds of LT2 and 3 (Fig. 3) and of armoured lapilli (Fig. 6B). Fragments of marine carbonate sediment and rock were quarried from the seafloor and incorporated in the flows. Removal of a substantial amount of carbonate mud created the accommodation space to allow entirely submarine deposition of the volcanic material. Subsequent and post-depositional subsidence triggered failure of the vent wall producing slumping and remobilization of tephra into the vent, which resulted in deposition of LT 1 and LT 4 (Fig. 6B).

## Acknowledgements

Many thanks are due to the people from the ODP depository for permission of access and sampling. A DFG-travel grant for C.B. to the depository at College Station, TX, is gratefully acknowledged. The KU Geology Associates travel funds for P.E. are greatly appreciated. Many thanks also to Michael Magnus and Alex Mock

(TU Bergakademie Freiberg) for introduction to image analysis. Constructive reviews by Kazuhiko Kano and James White helped to improve the manuscript appreciably. Helpful discussions with Karoly Nemeth about phreatomagmatism are greatly appreciated.

## References

- Batiza, R., 1989. Seamounts and seamount chains of the eastern Pacific. In: Winterer, E.L., Hussong, D.M., Decker, R. (Eds.), *The Eastern Pacific Ocean and Hawaii. The Geology of North America*, Geol. Soc. Am., Denver, CO, pp. 289–306.
- Batiza, R., Fornari, D.J., Vanko, D.A., Lonsdale, P., 1984. Craters, calderas, and hyaloclastites on young Pacific seamounts. *J. Geophys. Res.* 89, 8371–8390.
- Belousov, A., Belousova, M., 2001. Eruptive process, effect and deposits of the 1996 and the ancient basaltic phreatomagmatic eruptions in Karymakoye lake, Kamchatka, Russia. *Int. Assoc. Sedimentol. Spec. Publ.* 30, 35–60.
- Bograd, S.J., Rabinovich, A.B., LeBlond, P.H., Shore, J.A., 1997. Observations of seamount-attached eddies in the North Pacific. *J. Geophys. Res. – Oceans* 102, 12441–12456.
- Caplan-Auerbach, J., Duennebier, F., Ito, G., 2000. Origin of intraplate volcanoes from guyot heights and oceanic paleodepth. *J. Geophys. Res. – Solid Earth* 105, 2679–2697.
- Carmichael, I.S.E., 1979. Glass and the glassy rocks. In: Yoder, H.S. (Ed.), *The Evolution of Igneous Rocks*. Princeton University Press, Princeton, pp. 233–244.
- Carlsaw, H.S., Jaeger, J.C., 1947. *Conduction of Heat in Solids*. Clarendon Press, Oxford.
- Cashman, K.V., Fiske, R.S., 1991. Fallout of pyroclastic debris from submarine volcanic eruptions. *Science* 253, 275–280.
- Christie, D.M., Dieu, J.J., Gee, J.S., 1995. Petrologic studies of basement lavas from northwest Pacific guyots. In: Haggerty, J., Premoli Silva, I., Rack, F., McNutt, M.K. (Eds.), *Proceedings of the Ocean Drilling Program, Scientific Results 144*. Ocean Drilling Program, College Station, TX, pp. 495–508.
- Corcoran, P., 2000. Recognizing distinct proportions of seamounts using volcanic facies analysis: Examples from the Archean Slave Province, Northwest territories, Canada. *Precamb. Res.* 101, 237–261.
- Delesse, M.A., 1847. Procédé mécanique pour déterminer la composition des roches. *C. R. Acad. Sci.* 25, 544–545.
- Elf-Aquitaine, 1975. *Essai de caractérisation sédimentologique des dépôts carbonatés*. 172 pp.
- Fisher, R.V., 1961. Proposed classification of volcanoclastic sediments and rocks. *Geol. Soc. Am. Bull.* 72, 1395–1408.
- Fisher, R.V., 1977. Erosion by volcanic base-surge density currents: U-shaped channels. *Geol. Soc. Am. Bull.* 88, 1287–1297.
- Fisher, R.V., Schmincke, H.-U., 1984. *Pyroclastic Rocks*. Springer, Heidelberg, 474 pp.
- Fiske, R.S., Cashman, K.V., Shibata, A., Watanabe, K., 1998. Tephra dispersal from Myojinsho, Japan, during its shallow submarine eruption of 1952–1953. *Bull. Volcanol.* 59, 262–275.
- Fiske, R.S., Matsuda, T., 1964. Submarine equivalents of ash flows in the Tokiwa Formation, Japan. *Am. J. Sci.* 262, 76–106.
- Fornari, D.J., Malahoff, A., Heezen, B.C., 1978. Volcanic structure of the crest of the Puna Ridge, Hawaii: Geophysical implications of submarine volcanic terrain. *Geol. Soc. Am. Bull.* 89, 605–616.
- Francis, T.J.G., 1982. Thermal expansion effects in deep-sea sediments. *Nature* 299, 334–336.
- Gilbert, G.K., 1890. *Lake Bonneville*. United States Geological Survey Monograph 1, 438 pp.
- Goldhammer, R.K., 1997. Compaction and decompaction algorithms for sedimentary carbonates. *J. Sediment. Res.* 67, 26–35.
- Haq, B.U., Hardenbol, J., Vail, P.R., 1987. Chronology of fluctuating sea levels since the Triassic. *Science* 235, 1156–1167.
- Heiken, G., Wohletz, K., 1991. Fragmentation processes in explosive volcanic eruptions. In: Fisher, R., Smith, G. (Eds.), *Sedimentation in Volcanic Settings*. Society of Economic Paleontologists and Mineralogists, Special Publication 45, pp. 19–26.
- Higgins, M.D., 2002. Closure in crystal size distributions (CSD), verification of CSD calculations, and the significance of CSD fans. *Am. Mineral.* 87, 160–164.
- Hoffmeister, J.E., Ladd, H.S., Alling, H.L., 1929. Falcon Island. *Am. J. Sci.* 18, 461–471.
- Holmes, M.A., 1995. Pedogenic alteration of basalts recovered during leg 144. In: Haggerty, J., Premoli Silva, I., Rack, F., McNutt, M.K. (Eds.), *Proceedings of the Ocean Drilling Program, Scientific Results 144*, Ocean Drilling Program, College Station, TX, pp. 381–398.
- Houghton, B.F., Wilson, C.J.N., 1989. A vesicularity index for pyroclastic deposits. *Bull. Volcanol.* 51, 451–462.
- Jansa, L.F., Arnaud Vanneau, A., 1995. Carbonate buildup and sea-level changes at MIT Guyot, western Pacific. In: Haggerty, J., Premoli Silva, I., Rack, F., McNutt, M.K. (Eds.), *Proceedings of the Ocean Drilling Program, Scientific Results 144*, Ocean Drilling Program, College Station, TX, pp. 311–335.
- Kano, K., 1996. A Miocene coarse volcanoclastic mass-flow deposit in the Shimane Peninsula, SW Japan: product of a deep submarine eruption? *Bull. Volcanol.* 58, 131–143.
- Kano, K., 1998. A shallow-marine alkali-basalt tuff cone in the Middle Miocene Jinzai Formation, Izumo, SW Japan. *J. Volcanol. Geotherm. Res.* 87, 173–191.
- Knight, M.D., Jackson, M.C., et al., 1987. Volcanic evolution of the Koko Rift, southeastern Oahu, Hawaii. *Geological*

- Society of America, Cordilleran Section, 83rd Annual Meeting, Geological Society of America, Boulder, CO, 19, p. 395.
- Kokelaar, B.P., Durant, G.P., 1983. The submarine eruption of Surtla (Surtsey, Iceland). *J. Volcanol. Geotherm. Res.* 19, 239–246.
- Kokelaar, P., 1986. Magma–water interactions in subaqueous and emergent basaltic volcanism. *Bull. Volcanol.* 48, 275–289.
- Kokelaar, P., Busby, C., 1992. Subaqueous explosive eruption and welding of pyroclastic deposits. *Science* 257, 196–200.
- Koppers, A.A.P., Staudigel, H., Wijbrans, J.R., Pringle, M.S., 1998. The Magellan seamount trail: Implications for Cretaceous hotspot volcanism and absolute Pacific plate motion. *Earth Planet. Sci. Lett.* 163, 53–68.
- Kurnosov, V., Zolotarev, B., Eroshchev-Shak, V., Artomonov, A., Kashinzev, G., Murdma, I., 1995. Alteration of basalts from the west Pacific guyots, Legs 143 and 144. In: Haggerty, J., Premoli Silva, I., Rack, F., McNutt, M.K. (Eds.), *Proceedings of the Ocean Drilling Program, Scientific Results 144*, Ocean Drilling Program, College Station, TX, pp. 475–491.
- Lorenz, V., 1973. On the formation of Maars. *Bull. Volcanol.* 37, 183–204.
- Lorenz, V., 1974. Studies of the Surtsey tephra deposits. *Surtsey Res. Progr. Rep.* 7, 72–79.
- Martin, U., White, J.D.L., 2000. Depositional mechanisms of density current deposits from a submarine vent at the Otago Peninsula, New Zealand. In: Kneller, B., Peakall, J. (Eds.), *Sediment transport and deposition by particulate gravity currents*. *Int. Assoc. Sedimentol. Spec. Publ.* 33, pp. 245–259.
- McNutt, M.K., Fischer, K.M., 1987. The South Pacific super-swirl. In: Keating, B.H., Fryer, P., Batiza, R., Boehlert, G.W. (Eds.), *Seamounts, Islands, and Atolls*. American Geophysical Union, Monograph 43, pp. 25–34.
- McNutt, M.K., Winterer, E.L., Sager, W.W., Natland, J.H., Ito, G., 1990. The Darwin Rise: a Cretaceous super-swirl? *Geophys. Res. Lett.* 17, 1101–1104.
- McPhie, J., Doyle, M., Allen, R., 1993. *Volcanic Textures. A Guide to the Interpretation of Textures in Volcanic Rocks*. Tasmanian Government Printing Office, Tasmania, 196 pp.
- Miall, A.D., 1992. Exxon global cycle chart: An event for every occasion? *Geology* 20, 787–790.
- Nishimura, A., Rudolfo, K.S., Koizumi, A., Gill, J., Fujioka, K., 1992. Episodic deposition of Pliocene–Pleistocene pumice from the Izu–Bonoin arc, leg. 126. *Proc. Ocean Drilling Prog. Sci. Results* 126, 3–21.
- Ogg, J.G., 1995. MIT Guyot; depositional history of the carbonate platform from downhole logs at Site 878 (lagoon). In: Haggerty, J., Premoli Silva, I., Rack, F., McNutt, M.K. (Eds.), *Proceedings of the Ocean Drilling Program, Scientific Results 144*, Ocean Drilling Program, College Station, TX, pp. 337–359.
- Peacock, M.A., 1926. The petrology of Iceland, Part I. The basaltic tuffs. *Trans. R. Soc. Edinb.* 55, 51–76.
- Pringle, M.S., Duncan, R.A., 1995. Radiometric ages of basement lavas recovered at Loen, Wodejebato, MIT, and Ta-kuyo–Daisan Guyots, northwestern Pacific Ocean. In: Haggerty, J., Premoli Silva, I., Rack, F., McNutt, M.K. (Eds.), *Proceedings of the Ocean Drilling Program, Scientific Results 144*, Ocean Drilling Program, College Station, TX, pp. 547–557.
- Richards, A.F., 1959. Geology of the Islas Revillagigedo, Mexico, 1. Birth and development of Volcan Barcena, Isla San Benedicto. *Bull. Volcanol.* 22, 73–123.
- Rougerie, F., Fagerstrom, J.A., 1994. Cretaceous history of Pacific Basin guyot reefs – a reappraisal based on geothermal endo-upwelling. *Palaeogeogr. Palaeoclimatol. Palaeoecol.* 112, 239–260.
- Schumacher, R., Schmincke, H.-U., 1991. Internal structure and occurrence of accretionary lapilli – a case study at Laacher See Volcano. *Bull. Volcanol.* 53, 612–634.
- Shipboard Scientific Party, 1993. Site 878. In: Premoli Silva, I., Haggerty, J., Rack, F., et al., *Proceedings of the Ocean Drilling Program, Initial Reports 144*, Ocean Drilling Program, College Station, TX, pp. 331–412.
- Smellie, J.L., Hole, M.J., 1997. Products and processes in Pliocene–Recent, subaqueous to emergent volcanism in the Antarctic Peninsula: Examples of englacial Surtseyan volcano construction. *Bull. Volcanol.* 58, 628–646.
- Smith, W.H.F., Staudigel, H., Watts, A.B., Pringle, M.S., 1989. The Magellan Seamounts: Early Cretaceous record of the South Pacific isotopic and thermal anomaly. *J. Geophys. Res.* 94, 10501–10523.
- Sohn, Y.K., Chough, S.K., 1992. The Ichhulbong Tuff Cone, Cheju Island, South-Korea – Depositional processes and evolution of an emergent, Surtseyan-type tuff cone. *Sedimentology* 39, 523–544.
- Sohn, Y.K., 1995. Geology of Tok Island, Korea – Eruptive and depositional processes of a shoaling to emergent island volcano. *Bull. Volcanol.* 56, 660–674.
- Staudigel, H., Park, K.-H., Pringle, M.S., Rubenstone, J.L., Smith, W.H.F., Zindler, A., 1991. The longevity of the South Pacific isotopic and thermal anomaly. *Earth Planet. Sci. Lett.* 102, 24–44.
- Staudigel, H., Schmincke, H.-U., 1984. The Pliocene seamount series of La Palma/Canary Islands. *J. Geophys. Res.* 89, 11195–11215.
- Thorarinsson, S., 1967. *Surtsey: The New Island in the North Atlantic*. The Viking Press, New York, 47 pp.
- Thorarinsson, S., Einarsson, T., Sigvaldason, G., Elisson, G., 1964. The submarine eruption of the Vestmann Islands 1963–64: A preliminary report. *Bull. Volcanol.* 27, 435–445.
- White, J.D.L., 1991. Maar-diatreme phreatomagmatism at Hopi Buttes, Navajo Nation (Arizona), USA. *Bull. Volcanol.* 53, 239–258.
- White, J.D.L., 1996. Pre-emergent construction of a lacustrine basaltic volcano, Pahvant Butte, Utah (USA). *Bull. Volcanol.* 58, 249–262.
- White, J.D.L., Houghton, B.F., 2000. Surtseyan and related eruptions. In: Sigurdsson, H., Houghton, B., McNutt, S., Rymer, H., Stix, J. (Eds.), *Encyclopedia of Volcanoes*. Academic Press, New York, pp. 495–512.

- Winterer, E.L., 1976. Drilling into coral atolls. *Geotimes* 21, 20.
- Winterer, E.L., Natland, J.H., van Waasbergen, R.J., Duncan, R.A., McNutt, M.K., Wolfe, C.J., Premoli Silva, I., Sager, W.W., Sliter, W.V., 1993. Cretaceous guyots in the north-west Pacific: An overview of their geology and geophysics. In: Pringle, M.S., Sager, W.W., Sliter, W.V., Stein, S. (Eds.), *The Mesozoic Pacific: Geology, Tectonics, and Volcanism*. Geophysical Monograph, American Geophysical Union, Washington, DC, pp. 307–334.